



Monitoring the Effectiveness of Energy Consumption for Old Buildings Using Data Gathered Through Temperature, Humidity, and Light Intensity

John Reigton Hartono^{1*}, Ditdit Nugeraha Utama¹

¹ Computer Science Department, BINUS Graduate Program – Master of Computer Science, Bina Nusantara University, Jakarta, Indonesia.

Received: June 14, 2025

Revised: November 10, 2025

Accepted: December 25, 2025

Published: December 31, 2025

Corresponding Author:

John Reigton Hartono

john.hartono@binus.edu

DOI: [10.29303/jppipa.v11i12.11706](https://doi.org/10.29303/jppipa.v11i12.11706)

© 2025 The Authors. This open access article is distributed under a (CC-BY License)



Abstract: This research discusses the use of the Internet of Things in the monitoring of humidity, temperature, and light intensity conditions in a room that is connected to a mesh network. The objective of this research is to build a system that can monitor room conditions based on microcontrollers which are interconnected in a mesh network. The data are then displayed on a dashboard and categorized as either a comfortable or uncomfortable room based on existing standards. To ensure the accuracy of the system's values, it is compared to commercial tools, then accuracy and precision are calculated. The system's standard deviation for temperature is 0.12–0.19%, while its RMSE is 0.16–0.48%, and for humidity, the RMSE is 0.54–0.77%, with a standard deviation of 0.33–0.69%. For light intensity, with the outlier removed, the RMSE is 1.1–4.90% and the standard deviation is 0.79–2.76%. All these values are still comparable to the commercial tools' accuracy listed in specification sheets. For packet loss, the system is run continuously for nine days, and at the end, the total data sent and data received at the server are calculated to count the differences. The packet loss after nine days and 777,600 data points is 0.00103–0.00193% from all six sensors used in the system.

Keywords: Humidity; IoT; Mesh network; SDG 11; SDG 13

Introduction

Reducing dependence on fossil fuels has become a global imperative, especially in regions where access to renewable energy infrastructure remains limited (Sukmawati et al., 2022). One fundamental approach to supporting this transition involves minimizing unnecessary energy usage, such as by switching off lights and electronic devices when not in operation. However, energy efficiency becomes substantially more complex in the context of buildings, where consumption is concentrated in specific systems. Heating, ventilation, and air conditioning (HVAC) systems, along with lighting, represent the most significant contributors to building energy demand, accounting for approximately 38% and 20% of total usage, respectively (González-Torres et al., 2022; Hong & Rahmat, 2022). These

challenges are particularly pronounced in older buildings, which often lack energy-efficient construction materials and are typically not equipped to support contemporary energy monitoring and control technologies (Kim et al., 2019).

While simple steps like turning off lights remain important, a more comprehensive approach is needed. This can be achieved by installing systems that monitor HVAC and lighting usage in each room, providing real-time data on whether the air conditioning or lights are on. Implementing these practices will significantly reduce energy consumption, leading to lower costs and a reduced environmental impact from fossil fuel use (Zhao et al., 2023). However, a standard energy management system might not be ideal for older buildings. Instead, a self-contained system independent of the existing electrical network offers several

How to Cite:

Hartono, J. R., & Utama, D. N. (2025). Monitoring the Effectiveness of Energy Consumption for Old Buildings Using Data Gathered Through Temperature, Humidity, and Light Intensity. *Jurnal Penelitian Pendidikan IPA*, 11(12), 149–159. <https://doi.org/10.29303/jppipa.v11i12.11706>

advantages. This independence not only avoids compatibility issues but also allows the system to be easily expanded to serve more buildings (Carli et al., 2020). The more buildings that can be integrated, the greater the collective impact on energy savings and fossil fuel reduction (Zhang et al., 2023).

In older buildings with decentralized HVAC systems, mesh networking offers a viable solution for Internet of Things (IoT) implementation. Mesh networks consist of interconnected devices that communicate directly with each other, eliminating the need for a central router or server. This decentralized architecture allows for flexible deployment and adaptability to varying building configurations. Additionally, mesh networks increase reliability as each node communicates with others; if one node is removed or goes offline, other nodes can take its place as relays, ensuring the network remains functional (Jiang et al., 2021). Nevertheless, a good system goes beyond just being independent. It also needs to be accurate in monitoring room conditions. Users must have complete confidence in the system's readings to make informed decisions about energy use. Additionally, the system must reliably transmit data from each room to a central location. Data loss during transmission should be minimal to ensure users have complete information for making informed choices (Harb et al., 2022; Liu et al., 2020).

By integrating these energy-saving strategies with innovative technologies, people can revitalize older buildings. This approach not only reduces reliance on fossil fuels and lowers energy costs but also fosters a more sustainable future (Filippidou et al., 2019). The use of IoT for monitoring has gained substantial traction, particularly in industrial settings. However, prior research has primarily focused on industrial applications rather than domestic or indoor use cases. For example, IoT has been utilized in Industry 4.0 for predictive maintenance and in the construction industry through proprietary platforms and machine learning (Bertino et al., 2021). These methods often result in costly and inflexible systems, impeding their widespread adoption and limiting their effectiveness in combating climate change.

In the healthcare industry, IoT applications also face challenges, particularly in connecting devices to the internet. The most common solution involves Global System for Mobile Communications (GSM) for data transmission (Kulkarni et al., 2022). However, employing GSM for building monitoring can lead to inflated costs and inefficiencies, rendering it unsuitable for this purpose. Previous research has explored the use of multiple sensors, often employing Modbus for inter-sensor communication. This approach complicates network expansion and sensor addition, as it introduces additional costs. Other studies have utilized Universal

Asynchronous Receiver/ Transmitter (UART) for inter-sensor communication and connected a microcontroller to the internet via existing Wi-Fi networks. This method, however, is limited by the availability of Wi-Fi networks and requires an internet connection for operation.

LoRa (Long Range) has also been employed for inter-sensor communication before connecting to the internet via GSM. This approach is constrained by LoRa's limited Line of Sight (LOS) range, necessitating minimal obstructions between sensors. Additionally, Zigbee, a closed-source protocol requiring costly licenses, has been used. However, Zigbee is outdated and possesses security vulnerabilities. Mesh networks based on Wi-Fi protocols can address these issues.

Regarding controllers, some previous studies have replaced microcontrollers with Raspberry Pi. While this significantly enhances computational capabilities, these capabilities remain largely untapped, as Raspberry Pi is primarily used for sensor data acquisition and relay control. This approach also limits further network expansion due to Raspberry Pi's higher cost compared to microcontrollers like ESP8266 or ESP32.

Other research has employed Arduino Mega and the AT&T M2X protocol (Rahman et al., 2020). This microcontroller falls between Raspberry Pi and ESP32 in terms of capabilities. However, Arduino Mega 2560 lacks networking capabilities, necessitating an Ethernet HAT to connect sensors to the network before using the M2X protocol for internet access. This method introduces cabling complexities and limits scalability. The AT&T M2X protocol is also closed-source, proprietary, and relies on a third party (AT&T) for operation. Additionally, DHT11 is commonly used as a temperature and humidity sensor (Awaludin et al., 2021). This sensor employs one-wire protocol, which is known for its unreliability. Based on the author's experience, DHT11 sensors often fail to transmit data when used in systems with complex algorithms.

For light sensing, some previous studies have utilized LDRs (Light Dependent Resistors). These sensors rely on resistance to detect light intensity, necessitating pre-calibration before use. While less expensive than BH1750 sensors, LDRs are unreliable due to temperature sensitivity and slow response times caused by light-induced chemical reactions (Casals et al., 2020).

To address the limitations of existing IoT monitoring systems, this research proposes a novel system utilizing ESP32 microcontrollers, AHT10 temperature and humidity sensors, and BH1750 light intensity sensors. The proposed system offers several advantages over previous works, one of which is the reliability of the new sensors running on I2C communication and a mesh network based on Wi-Fi.

Old buildings often suffer from outdated design and construction methods that do not align with modern standards of energy efficiency. These structures typically have poor insulation, inefficient heating and cooling systems, and limited integration with smart technologies. As global concerns over energy consumption and environmental sustainability increase, there is an urgent need to improve the energy performance of existing buildings, particularly those of historical or functional importance. Monitoring environmental parameters such as temperature, humidity, and light intensity provides essential data to evaluate energy use patterns, detect inefficiencies, and guide retrofitting strategies. Without effective monitoring, efforts to reduce energy consumption in old buildings risk being inefficient or misdirected, leading to higher operational costs and environmental impact. This study introduces a novel approach by integrating real-time environmental data specifically temperature, humidity, and light intensity to assess the effectiveness of energy usage in old buildings. While previous research has focused largely on theoretical models or energy audits, this study emphasizes empirical, sensor-based monitoring to capture the dynamic environmental behavior of aging structures. The innovation lies in using this real-time data to create a responsive and adaptive framework for energy management that is both low-cost and scalable. This method not only provides a more accurate understanding of energy performance but also enables practical interventions tailored to the specific environmental context of each building.

Method

The device is built using an ESP32 as the control unit. The ESP32 was chosen because the ESP8266 was not designed with mesh networking in mind. The mesh networking implementation and data transmission follow the research of Aquino et al. (2021) and are adapted to the sensors used. The sensors used in this research are AHT10 and BH1750. These sensors use Inter-Integrated Circuit (I2C) communication to address communication problems with DHT11. BH1750 uses a photodiode to sense light intensity, which addresses temperature-related problems associated with LDRs. These sensors are then connected to the ESP32 microcontroller, and each ESP32 microcontroller is connected to others using a mesh network. This mesh network is extended to the server, and the data are handled using the MQTT protocol via the Mosquitto Broker. The data are then distributed to Node-RED before being stored in a CSV file and displayed on the dashboard. This process is illustrated in Figure 1.

Before the experiment began, a $30 \times 30 \times 30$ cm cardboard box was prepared as the testing medium. Two types of testing media were created: one for temperature and humidity testing, and the other for light intensity testing.

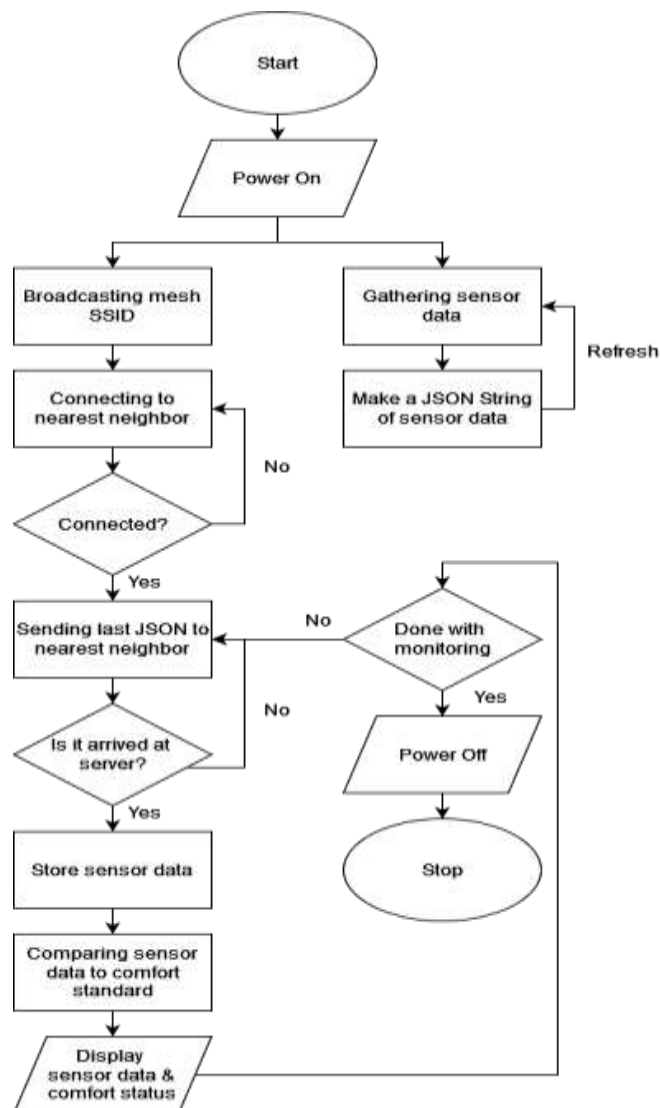


Figure 1. Overview of the suggested system

For temperature and humidity testing, the testing media were made with holes on the left and right sides for water to enter and exit, and another hole for the power cable to exit. Inside the testing media box, a 300 W thermoelectric cooler was placed with the cold side in contact with a heatsink equipped with a fan, while the hot side was in contact with a water block that was circulated with water by a pump. Both the pump and the Peltier cooler were connected to a power supply that was set with a timer to cool for five minutes and heat for five minutes.

This testing medium can be seen in Figure 2. In the upper left part, the position of the commercial device and sensors can be seen during the preparation for measurement. In the upper right part, the placement of the Peltier cooler can be seen, and in the lower part, it can be seen that when the testing media box is closed, the power supply and timer are on top of the box, and the pump is on the side.



Figure 2. Temperature and humidity measuring medium

For light intensity testing, an 8x8 LED matrix was attached to the top of the testing media box. The LED matrix was connected to an ESP8266 microcontroller that controlled the lighting level from 256 brightness levels, changing from 0 to 255 over 5 minutes and from 255 to 0 over 5 minutes.

This testing medium can be seen in Figure 3. On the left, the light source, sensors, and commercial device can be seen placed for testing. Once arranged, the testing media box is closed, and measurements are taken. On the upper right, the sensors are placed on a 3D-printed bracket that ensures the sensors are at the same distance from each other. On the lower right, the light source from the LED matrix controlled by the ESP8266 can be seen.

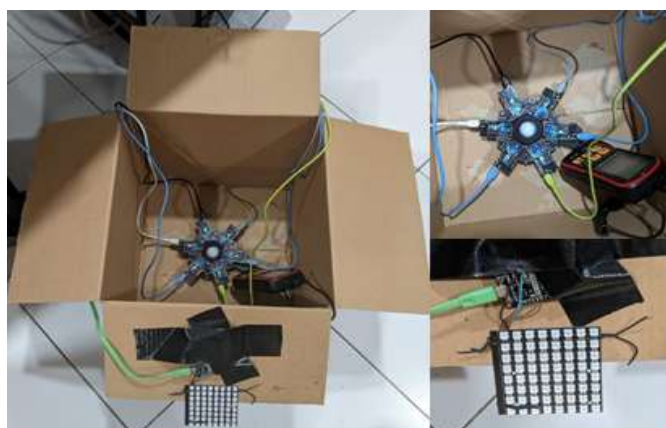


Figure 3. Light intensity measuring medium

The ground truth used in this experiment is the Benetech GM1030 for light intensity and the Benetech GM1360A for temperature and humidity. The sensors were compared to these two commercial tools to assess their performance. These sensors were placed inside the testing medium according to the tested parameters.

For testing packet loss, the devices were placed in six rooms, and every device sent data every second to the Raspberry Pi server. This was done for nine days, and the average loss for every device was observed. The amount of data received by the server was compared to the amount of data sent by using time as a reference. This experiment was conducted in a room with gypsum walls. The devices were distributed in six rooms with an average distance of 6 m, arranged in three columns and two rows, as shown in Figure 4.

Room 1	Room 2	Room 3
Room 4	Room 5	Room 6

Figure 4. Six rooms used for testing package loss

All data were then evaluated in three categories: accuracy of the system by calculating the Root Mean Square Error (RMSE) of each device, precision by calculating the standard deviation of each device, and finally, evaluating network capability by counting packet loss. The accuracy of the data was evaluated by calculating the RMSE compared to a commercial device. RMSE is a statistical measure of the average difference between the predicted values and the actual values. A lower RMSE value indicates a more accurate system. In the case of temperature and humidity data, the RMSE was calculated by comparing the temperature and humidity readings from the system's sensors to the readings from the commercial device. The RMSE was calculated for every second and then averaged over the entire 100-cycle test period. For light intensity data, the RMSE was calculated by comparing the light intensity readings from the system's sensors to the light intensity readings from the commercial device. The RMSE was calculated for every second and then averaged over the entire 100-cycle test period.

Data precision was assessed by calculating the standard deviation in comparison to a commercial device. Standard deviation measures the dispersion of data points from the mean, with a lower value indicating higher precision. For temperature and humidity data, the standard deviation was calculated from the sensor readings at each second and averaged over the entire

100-cycle test period. The same approach was used for light intensity data, with standard deviation calculated for each second and averaged over the 100-cycle period.

Data loss was determined by counting the number of data packets that were not received by the Raspberry Pi. This data loss is expressed as a percentage of the total packets sent, with a lower percentage indicating a more reliable system. The data loss calculation was based on nine days of data, totalling nearly 800,000 packets per node. For data management and visualization, Node-RED is utilized. A Node-RED dashboard logs sensor data into a CSV file, with a function that appends time and date columns to the data received from the MQTT broker before saving it to the file. The CSV file is then saved to the Raspberry Pi for further analysis. This data flow is translated into a Node-RED flow, as shown in Figure 5.



Figure 5. Flow on node-red for storing sensor data

Data for each room are presented on a dashboard within a single sheet. The data, received from the MQTT node, are divided into six outputs: three are displayed as gauges, and three as text. For the text outputs, the ISO CIE 8995-2002 and OSHA 1910.1000 room standards are utilized. The process flow is illustrated in Figure 6. A workspace is deemed comfortable if it meets the following conditions: light levels exceed 200 lux, temperature ranges from 19.5 °C to 27.8 °C, and humidity remains below 65%. Figure 6 shows the flow of the dashboard, while Figure 7 shows the dashboard itself.

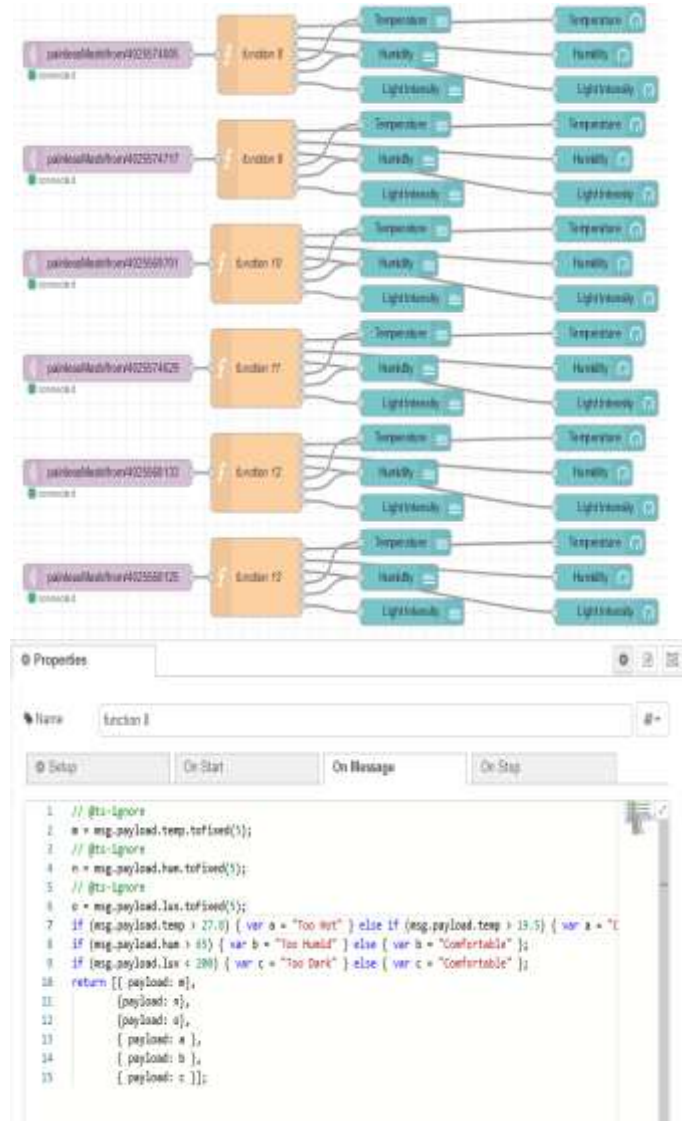


Figure 6. Flow of the node-red dashboard



Figure 7. Appearance of the dashboard

If the sensor reading is not up to standard each text on top of the gauge for every room will notify the user about the condition. The color of the gauge itself will

change according to the value of sensor reading compared to the standard used.

Results and Discussion

Testing Sensor for Light Intensity

In contrast to temperature and humidity measurements, light intensity is affected by the centralized light source within a relatively small area compared to the measurement room. The light intensity value will vary based on the distance from the source to the sensor, with higher light intensity values decreasing quadratically as the distance from the light source increases.

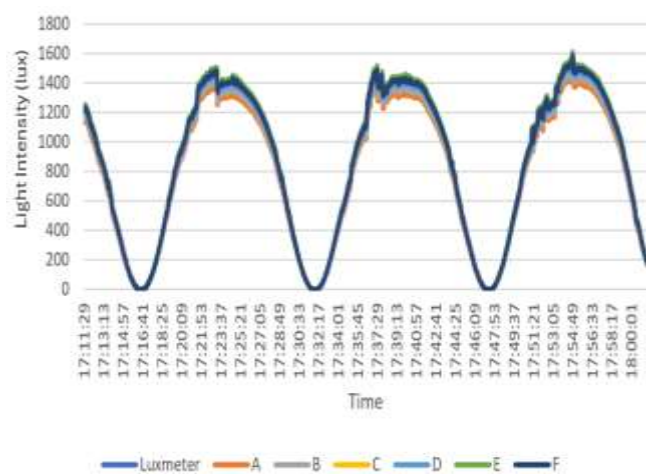


Figure 8. The first 3000 data of light intensity against time from all 6 sensors

This variation in sensor placement results in differing intensity readings across sensors. As illustrated in Figure 8, although the sensors generally follow the trend of the reference sensor, discrepancies become more pronounced at higher light intensities due to the varying sensor positions. Figure 8 displays the initial 3000 data points from all six sensors. When the light source is observed to undergo irregular changes, each sensor measures the change with the same trend direction. If the Pearson correlation is calculated between the commercial reference lux meter and each sensor, the values in

Table 1 are obtained.

Table 1 indicates that the readings from each sensor are highly correlated with those from the reference device. To assess the error, the RMSE for each sensor is calculated. Percentages are used for RMSE values to account for the large range of measurements, which span from a minimum of 0 to over 1,600 lux. This approach ensures that the error values effectively reflect the accuracy of the sensors across all measurement levels used in the experiment.

Table 1. Table of R Value from Light Intensity Data

	R Value
Sensor A	0.998696
Sensor B	0.999435
Sensor C	0.999717
Sensor D	0.999907
Sensor E	0.999115
Sensor F	0.999770

Table 2 demonstrates significant variability in error values. This variation arises from the light source's use of a PWM mechanism for dimming and turning the light on and off. In very dark conditions, even minor changes in sensor readings can lead to substantial errors. Additionally, each sensor records data at slightly different times, though for consistency, the data are aggregated into one reading per second. Both the PWM mechanism and the consolidation of data into single-second intervals contribute to high error percentages in some sensor readings, resulting in numerous outliers. These outliers become evident when a boxplot is created for all 100,000 data points.

Table 2. RMSE and Standard Deviation of Light Intensity Compared to Commercial Tools

	RMSE	Standard deviation
Sensor A	4.59%	3.97%
Sensor B	6.31%	4.44%
Sensor C	3.91%	2.76%
Sensor D	2.34%	2.18%
Sensor E	4.78%	4.78%
Sensor F	1.77%	1.70%

Table 2 indicates that both the standard deviation and RMSE are relatively high. To better understand this, the data are visualized in Figure 9 using a boxplot on the left. This plot reveals a considerable spread in the data, highlighting the need for cleanup. Outliers from each sensor, identified using the interquartile range (IQR), were removed. The cleaned data are then visualized again, as shown on the left side of Figure 9.

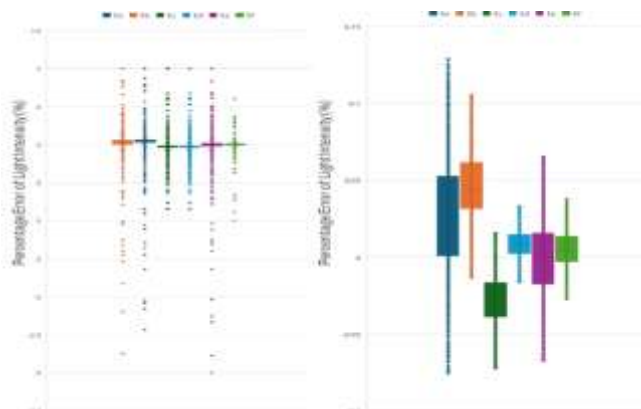


Figure 9. Data of light intensity before removing outlier and after

Both RMSE and standard deviation are much better than before the outliers were removed, but for sensor B, RMSE still exceeds the reference value of $\pm 4\%$ error. This value would be much better if the light source intensity were controlled using voltage or current rather than Pulse Width Modulation (PWM).

Table 3. RMSE and Standard Deviation of Light Intensity after Outlier Removed

	RMSE	Standard Deviation
Sensor A	3.59%	2.76%
Sensor B	4.90%	1.95%
Sensor C	3.12%	1.47%
Sensor D	1.17%	0.79%
Sensor E	2.25%	2.25%
Sensor F	1.25%	1.14%

LEDs were chosen because they are relatively inexpensive and easier to set up than using current and voltage. LEDs can also be controlled more precisely for voltages or currents within the working voltage or current range. In addition to the light source, the placement of the sensors also greatly affects the values read by each sensor. As can be seen from Figure 8, there is always a deviation among sensors. If the sensor placement is the same, this deviation can be reduced. However, according to the literature, the change in light that can be perceived by humans is 7.4%. The error value and standard deviation are still below this threshold, which shows that the BH1750 sensor can still be used for everyday indoor applications.

Testing Sensor for Temperature

Out of the 100,000 data points that were taken, 1,000 data points were visualized in Figure 10 to see the difference between each sensor and the reference temperature. It can be seen that the difference in the values read is not far off. To clarify the difference in the values read, a boxplot was then created for the entire 100,000 data points that were taken.

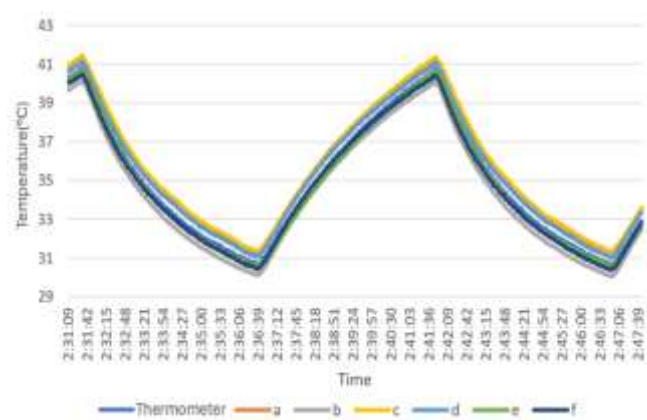


Figure 10. The first 1000 data of temperatur against time from all 6 sensors

Figure 10 shows the difference in sensor values compared to the reference. Since this boxplot was created with all 100,000 data, the values displayed represent the entire population of data measured by the 6 sensors. From this boxplot, it can be seen that the data distribution of each sensor is quite small, which is represented by the standard deviation value of less than 1%. The calculation of the standard deviation for each sensor is shown in Table 4.

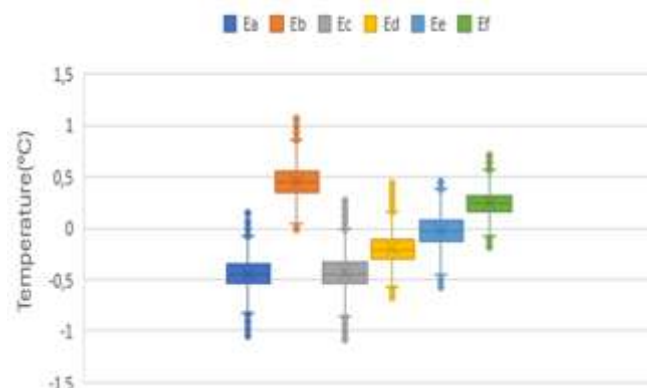


Figure 11. Boxplot of all 100.000 of temperature data from all 6 sensor

Table 4. RMSE and Standard Deviation of Temperature

	RMSE	Standard Deviation
Sensor A	0.47%	0.15%
Sensor B	0.48%	0.14%
Sensor C	0.47%	0.19%
Sensor D	0.26%	0.16%
Sensor E	0.16%	0.16%
Sensor F	0.27%	0.12%

Referring to the boxplot in Figure 11, which shows the temperature distribution, it can be seen that the distribution value is still below $\pm 1^{\circ}\text{C}$, with some outliers of -1.03°C , 1.06°C , and 1.07°C in sensors A, B, and C, respectively. In addition, all of these are still comparable to the commercial reference device used.

The RMSE of each sensor is not worse than that of the reference device, which is a maximum of $\pm 1^\circ\text{C}$. With a standard deviation of less than 0.2°C and an RMSE of less than 0.5°C , the AHT10 sensor is considered sufficient for measuring room temperature. This refers to²⁷ where a temperature change of 0.92°C ($\pm 0.05^\circ\text{C}$) can be perceived by humans with 95% accuracy.

Testing Sensor for Humidity

Temperature and humidity are highly dependent on each other. The relative humidity value depends on the current temperature because the ability of air to bind water vapor depends on the air temperature. The higher the air temperature, the greater the capacity of air to bind water vapor. If the amount of water vapor in the air is constant, the relative humidity value will decrease if the temperature rises, and vice versa.

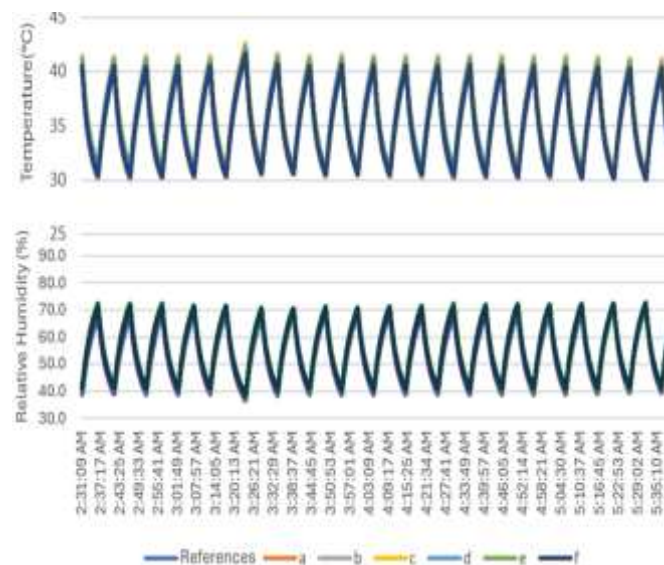


Figure 12. Value of temperature and humidity at the same time

The top portion of Figure 12 shows the humidity values read by the 6 sensors over time. The graph shows 10 hours or 36,000 data points so that the trend of the relationship between temperature and humidity can be seen. The humidity value is change with the changes in the temperature value in the opposite direction (Laura et al., 2023).

After ensuring that the sensors are functioning, the accuracy and precision of the sensors are then determined by calculating the RMSE and standard deviation of the sensors. The RMSE and standard deviation are calculated from the data that has been collected and written down in Table 5.

Table 5. RMSE and Standard Deviation of Humidity

	RMSE	Standard deviation
Sensor A	1.260886	0.334768

Sensor B	1.773866	0.470935
Sensor C	1.223893	0.403527
Sensor D	0.544912	0.342023
Sensor E	0.693869	0.689724
Sensor F	1.062222	0.330923

Table 5 shows that Sensor D, with an RMSE of 0.545%, has the best value among all sensors. However, all sensors still have values below 3%. Three percent is used as a reference because the Benetech GM1360A reference device has an accuracy of $\pm 3\%$.

To see the level of precision of this humidity measurement, a boxplot is created, as shown in Figure 13.

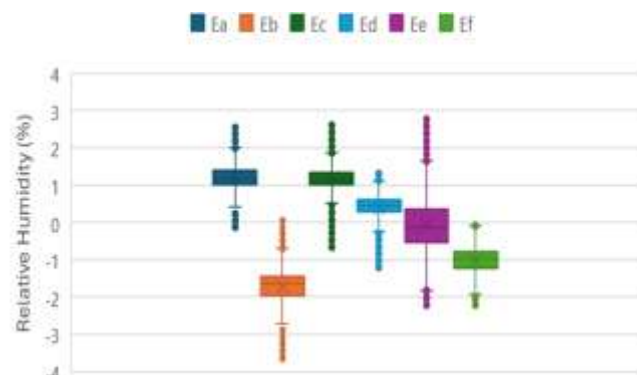


Figure 13. Boxplot of all 100.000 of temperature data from all 6 sensors

Figure 13 illustrates the distribution of error for each sensor, with sensor E exhibiting the widest spread. This observation aligns with the earlier standard deviation calculation, which indicated that sensor E has the highest standard deviation value.

Testing for Data Loss

To minimize disruption to daily operations at the building where the data was collected, data collection was scheduled from December 23, 2023, to January 2, 2024. During this period, data was gathered for 9 days, totaling nearly 780,000 samples.



Figure 14. Number of packets loss sample every 12 hours for all 6 sensors

The data were sampled every 12 hours to record the transmission time, which was then compared to the reference time. If the recorded time was earlier than the reference time, it indicated that packets were lost and data entries were missed. Each missed second corresponded to one lost packet. As shown in Table 6, the packet loss does not follow a fixed pattern but results in an overall loss rate of 0.00103%, or approximately 1 packet lost per 100,000 transmissions.

For sensor B, as indicated in Table 6, the packet loss at the end of day 9 was 0.00193%, which is higher than the 0.00103% observed for sensor A. This difference may be attributed to variations in the sensors' operational environments. Sensor C, as shown in Table 6, had a packet loss of 0.00129%, falling between the values of sensor A and sensor B. Sensor D's packet loss was 0.00167%, which is close to the values for the other three sensors, positioning it between sensor A, with the lowest packet loss, and sensor B, with the highest.

Table 6. Packets Loss after 777.600 Data Sent

	Percentage Packets Loss
Sensor A	0.00103%
Sensor B	0.00193%
Sensor C	0.00129%
Sensor D	0.00167%
Sensor E	0.00167%
Sensor F	0.00180%

The data from sensor E, as shown in Table 6, indicates a packet loss percentage identical to that of sensor D. However, sensor E reached this packet loss value first, at data point 734,400, as illustrated in Figure 14. Sensor F's data, also depicted in Figure 14, shows a trend similar to sensor E's but experienced one additional lost packet in the last 12 hours, resulting in a slightly higher packet loss percentage of 0.00180% compared to sensor E. This packet loss rate is significantly lower than the 1% threshold commonly used for acceptable levels in Voice over Internet Protocol (VoIP). Unlike VoIP, which requires continuous data transmission, temperature and humidity monitoring does not need such continuous data collection. Therefore, the observed packet loss levels are considered acceptable for this monitoring system.

These results align with prior studies that emphasize the viability of wireless sensor networks (WSNs) in environmental monitoring with minimal data loss. For example, research conducted on smart building monitoring systems using Zigbee-based WSNs reported packet loss rates averaging 0.002% under stable indoor conditions, which is slightly higher than those observed

in this study (Márquez, 2021). This suggests that the communication protocol and hardware configuration used in the present system are at least equally efficient, if not superior, in maintaining data integrity.

Furthermore, a study evaluating packet reliability in IoT-based HVAC monitoring found that packet loss often increases during peak operational hours due to electromagnetic interference and network congestion, especially in older buildings with thick walls or metal reinforcements (Kychkin et al., 2021). In contrast, our study observed a consistent and minimal packet loss over time, even in an older building setting, indicating the robustness of the implemented sensor deployment and network topology. This stability is particularly valuable in heritage or aging infrastructure, where the integration of monitoring technology often faces physical constraints.

Notably, the packet loss rates in this study are far below the commonly referenced 1% threshold applied in latency-sensitive applications such as VoIP (Mohd Ali et al., 2021). While real-time applications require near-zero tolerance for loss, environmental monitoring particularly of parameters like temperature, humidity, and light intensity can accommodate minor data gaps without affecting the reliability of long-term trend analysis.

In summary, compared to existing literature, the present system demonstrates enhanced reliability with negligible data loss, validating its suitability for energy consumption monitoring in older buildings. These findings support broader adoption of similar low-power, high-efficiency sensor networks for building energy analysis, particularly where retrofitting modern infrastructure is not feasible.

Conclusion

Based on the experiments, a monitoring system for light intensity, temperature, and humidity can be effectively implemented using ESP32, AHT10, and BH1750 sensors. This system operates independently of existing wireless networks by utilizing mesh networking. Over the nine-day period and 777,600 data points collected, packet loss ranged from 0.00103% to 0.00193%. The sensors used in this experiment show comparable performance to commercial tools. Specifically: for temperature, the AHT10 sensor has an RMSE ranging from 0.16% to 0.48% and a standard deviation from 0.12% to 0.19%. For humidity, the RMSE ranges from 0.54% to 1.77%, with a standard deviation between 0.33% and 0.69%. For light intensity, due to the PWM-based nature of the experiment, values can be erratic. After removing outliers, the RMSE ranges from 1.1% to 4.90%, with a standard deviation from 0.79% to 2.76%. All these values remain within the acceptable

tolerance levels of commercial tools' accuracy and precision.

Acknowledgments

The authors would like to express their sincere gratitude to all individuals and institutions that contributed to the completion of this study.

Author Contributions

Conceptualization, J.R.H.; methodology, D.N.U; software, J.R.H.; validation, D.N.U.; formal analysis, J.R.H.; investigation, J.R.H.; resources, J.R.H; data curation, D.N.U.; writing—original draft preparation, J.R.H.; writing—review and editing, J.R.H.; visualization J.R.H.; supervision, D.N.U.; project administration, N.S.; funding acquisition, D.N.U.

Funding

This research received no external funding.

Conflicts of Interest

The authors declare that they have no known competing financial interests or personal relationships that could have appeared to influence the work reported in this paper.

References

Aquino, A. G. Q., Ballado, A. H., & Bautista, A. V. (2021). Implementing a Wireless Sensor Network with Multiple Arduino-Based Farming Multi-Sensor Tool to Monitor a Small Farm Area Using ESP32 Microcontroller Board. *2021 IEEE 13th International Conference on Humanoid, Nanotechnology, Information Technology, Communication and Control, Environment, and Management, HNICEM 2021*. <https://doi.org/10.1109/HNICEM54116.2021.9731989>

Awaludin, M., Rangan, A. Y., & Yusnita, A. (2021). Internet of Things (IoT) Based Temperature and Humidity Monitoring System in the Chemical Laboratory of the Samarinda Industry Standardization and Research Center. *Tepian*, 2(3), 85-93. <https://doi.org/10.51967/tepi.v2i3.344>

Bertino, E., Jahanshahi, M. R., Singla, A., & Wu, R. T. (2021). Intelligent IoT systems for civil infrastructure health monitoring: a research roadmap. *Discover Internet of Things*, 1(1). <https://doi.org/10.1007/s43926-021-00009-4>

Carli, R., Cavone, G., Othman, S. Ben, & Dotoli, M. (2020). IoT based architecture for model predictive control of HVAC systems in smart buildings. *Sensors (Switzerland)*, 20(3). <https://doi.org/10.3390/s20030781>

Casals, M., Gangoheels, M., Macarulla, M., Forcada, N., Fuertes, A., & Jones, R. V. (2020). Assessing the effectiveness of gamification in reducing domestic energy consumption: Lessons learned from the EnerGAware project. *Energy and Buildings*, 210. <https://doi.org/10.1016/j.enbuild.2019.109753>

Filippidou, F., Nieboer, N., & Visscher, H. (2019). Effectiveness of energy renovations: a reassessment based on actual consumption savings. *Energy Efficiency*, 12(1). <https://doi.org/10.1007/s12053-018-9634-8>

González-Torres, M., Pérez-Lombard, L., Coronel, J. F., Maestre, I. R., & Yan, D. (2022). A review on buildings energy information: Trends, end-uses, fuels and drivers. *Energy Reports*, 8, 626-637. <https://doi.org/10.1016/j.egyr.2021.11.280>

Harb, H., Nader, D., Sabeh, K., & Makhoul, A. (2022). Real-time Approach for Decision Making in IoT-based Applications. *Proceedings of the 11th International Conference on Sensor Networks*, 223-230. <https://doi.org/10.5220/0010985800003118>

Hong, W. Y., & Rahmat, B. N. N. N. (2022). Energy consumption, CO2 emissions and electricity costs of lighting for commercial buildings in Southeast Asia. *Scientific Reports*, 12(1). <https://doi.org/10.1038/s41598-022-18003-3>

Jiang, X., Zhang, H., Barsallo Yi, E. A., Raghunathan, N., Mousoulis, C., Chaterji, S., Peroulis, D., Shakouri, A., & Bagchi, S. (2021). Hybrid Low-Power Wide-Area Mesh Network for IoT Applications. *IEEE Internet of Things Journal*, 8(2), 901-915. <https://doi.org/10.1109/JIOT.2020.3009228>

Kim, D. B., Kim, D. D., & Kim, T. (2019). Energy performance assessment of HVAC commissioning using long-term monitoring data: A case study of the newly built office building in South Korea. *Energy and Buildings*, 204. <https://doi.org/10.1016/j.enbuild.2019.109465>

Kulkarni, P. M., Parvekar, V., Nagpure, P., Mhoprekar, S., Mudawadkar, G., Nandurkar, S., & Hande, N. (2022). IOT Based Health Monitoring System. *International Journal for Research in Applied Science and Engineering Technology*, 10(12), 803-808. <https://doi.org/10.22214/ijraset.2022.48022>

Kychkin, A. V., Gorshkov, O. V., Selivanov, V. A., & Pavlov, V. A. (2021). Technology for the soft implementing a digital twin into the IoT HVAC control loop. *Journal Of Applied Informatics*, 16(95). <https://doi.org/10.37791/2687-0649-2021-16-5-33-47>

Laura, B., Andrea, V., Massimiliano, Z., & Riccardo, P. (2023). An investigation on humans' sensitivity to environmental temperature. *Scientific Reports*, 13(1). <https://doi.org/10.1038/s41598-023-47880-5>

Liu, G. X., Shi, L. F., & Xin, D. J. (2020). Data Integrity Monitoring Method of Digital Sensors for Internet-of-Things Applications. *IEEE Internet of Things Journal*, 7(5), 4575-4584. <https://doi.org/10.1109/JIOT.2020.2967504>

Márquez, F. P. G. (2021). Introductory Chapter: Internet of Things. In *Internet of Things*.

<https://doi.org/10.5772/intechopen.98268>
Mohd Ali, A., Dhimish, M., Alsmadi, M. M., & Mather, P. (2021). An Algorithmic Approach to Identify the Optimum Network Architecture and WLAN Protocol for VoIP Application. *Wireless Personal Communications*, 119(4).
<https://doi.org/10.1007/s11277-021-08383-6>

Rahman, R. A., Hashim, U. R. A., & Ahmad, S. (2020). IoT based temperature and humidity monitoring framework. *Bulletin of Electrical Engineering and Informatics*, 9(1), 229–237. Retrieved from <https://www.beei.org/index.php/EEI/article/view/1557>

Sukmawati, E., Adhicandra, I., Sucahyo, N., Ayuningtyas, A., & Nurwijayanti, K. N. (2022). Information System Design of Online-Based Technology News Forum. *International Journal Of Artificial Intelligence Research*, 1(2).
<https://doi.org/10.29099/ijair.v6i1.2.593>

Zhang, F., Saeed, N., & Sadeghian, P. (2023). Deep learning in fault detection and diagnosis of building HVAC systems: A systematic review with meta analysis. In *Energy and AI* (Vol. 12).
<https://doi.org/10.1016/j.egyai.2023.100235>

Zhao, D., Watari, D., Ozawa, Y., Taniguchi, I., Suzuki, T., Shimoda, Y., & Onoye, T. (2023). Data-driven online energy management framework for HVAC systems: An experimental study. *Applied Energy*, 352.
<https://doi.org/10.1016/j.apenergy.2023.121921>